

# Structure and interaction potentials in solid-supported lipid membranes studied by X-ray reflectivity at varied osmotic pressure

Ulrike Mennicke<sup>a</sup>, Doru Constantin<sup>b</sup>, and Tim Salditt<sup>c</sup>

Institut für Röntgenphysik, Friedrich-Hund-Platz 1, 37077 Göttingen, Germany

August 15, 2018

**Abstract.** Highly oriented solid-supported lipid membranes in stacks of controlled number  $N \simeq 16$  (oligo-membranes) have been prepared by spin-coating using the uncharged lipid model system 1,2-dimyristoyl-sn-glycero-3-phosphocholine (DMPC). The samples have been immersed in aqueous polymer solutions for control of osmotic pressure and have been studied by X-ray reflectivity. The bilayer structure and fluctuations have been determined by modelling the data over the full  $q$ -range. Thermal fluctuations are described using the continuous smectic hamiltonian with the appropriate boundary conditions at the substrate and at the free surface of the stack. The resulting fluctuation amplitudes and the pressure-distance relation are discussed in view of the inter-bilayer potential.

**PACS.** 61.10.Kw X-ray reflectometry (surfaces, interfaces, films) – 87.16.Dg Membranes, bilayers, and vesicles – 87.15.Ya Fluctuations

## 1 Introduction

A quantitative understanding of the structure, fluctuations, interaction potential and elasticity properties of lipid membranes, which represent model systems for biological membranes, has been the goal of many theoretical and experimental studies. Theoretically, they have been studied as paradigmatic examples of quasi two-dimensional macromolecular structures governed by bending rigidity [1]. In aqueous solution, lipid bilayers assemble into stacks governed by distinct inter-bilayer interactions. A number of seminal studies using high resolution synchrotron X-rays have been published on these systems [2,3,4,5]. In these studies, isotropic aqueous dispersions of multilamellar vesicles have been studied as a function of temperature  $T$  and/or osmotic pressure  $\Pi$ . Detailed quantitative information on the interaction potentials and the elasticity properties has thus been derived, see *e.g.* [2,3,4]. However, information is lost in these small-angle scattering studies due to crystallographic powder averaging. In the analysis, assumptions must therefore be made on the nature of the correlation functions in the framework of linear smectic elasticity theory, leading to the Caillé model [6] and related theories, see for instance [7]. In order to overcome the limitations of powder averaging, it is desirable

to work with aligned systems of lipid bilayers [8,9,10,11,12]. Under the same conditions of temperature and hydration, thermal fluctuations are not as strong for aligned systems as in bulk studies due to the boundary condition at the flat substrate, enabling a higher resolution in  $\rho(z)$ . It is also advantageous to fit the data continuously over a large range of momentum transfer  $q$ , as has been shown for isotropic solutions [5] and for oriented stacks [12], and not only in the vicinity of the Bragg peaks arising from the multilamellar structure. However, for aligned systems of multilamellar membranes, satisfactory fits of the entire reflectivity curves and the formulation of a proper statistical model as well as of a scattering theory are still quite difficult. Note that the best published fits are for systems consisting of monolayers at the air-water interface, for single bilayers or for a free-floating bilayer system developed by Fragneto and coworkers [13]. In multilamellar systems on the other hand, the reflectivity signal is typically much more complex and structured. As we show here, structural parameters of the bilayer, interaction and fluctuation parameters can be deduced from these curves, and are compared with the literature.

Most previous studies on aligned multilamellar membranes suffered from a lack of control concerning the number of bilayers  $N$ , the sample homogeneity and also the bilayer hydration. Building on recent progress in the preparation of bilayers on solid support by spin-coating [14], we use so-called oligo-membranes with a reduced number of bilayers  $N \simeq 10 - 20$  resulting in very structured and well resolved reflectivity signals. We have developed

<sup>a</sup> e-mail: [ulrike.mennicke@gmx.net](mailto:ulrike.mennicke@gmx.net)

<sup>b</sup> e-mail: [constantin@lps.u-psud.fr](mailto:constantin@lps.u-psud.fr) Permanent address: Laboratoire de Physique des Solides, Université Paris-Sud, Bât. 510, 91405 Orsay Cedex, France.

<sup>c</sup> e-mail: [tsaldit@gwdg.de](mailto:tsaldit@gwdg.de)

a model for the thermal fluctuations calculated for the proper boundary conditions (rigid substrate and free upper surface), which gives the fluctuation amplitudes  $\langle u_n^2 \rangle$  of the bilayers as a function of their position in the stack,  $n = \overline{1, N}$ . The values for  $\langle u_n^2 \rangle$  are then inserted in the multilamellar structure factor, along with a decreasing coverage function (see below). The density profile  $\rho(z)$  is parameterized in terms of its Fourier coefficients [15]. This approach gives for the first time an agreement with the measured reflectivity curve of multilamellar membranes over the full range of  $q_z$  up to typically  $q_z \simeq 0.7 \text{ \AA}^{-1}$  and over about seven orders of magnitude in the measured signal.

The main experimental parameter in this study is the osmotic pressure. The classical osmotic stress (OS) technique as developed by Parsegian and coworkers [16] is widely used for the measurement of force-distance curves in colloidal systems. The osmotic pressure imposed to a lamellar phase controls the interaction force experienced by the membranes across the water layer by setting the chemical potential of the water molecules in the inter-bilayer solution. Pressure-distance relations can be easily determined, *e.g.* if the lamellar periodicity  $d$  is measured by X-ray scattering at different pressures  $\Pi$ .

In this study we use a variant of the OS technique where the oriented bilayers are put in direct contact with the osmotic stress solution [18]. We have verified that the high molecular weight polymer with a radius of gyration larger than  $d$  does not penetrate the lamellar phase. We emphasize that the osmotic pressure is one of the most important parameters in biomolecular systems, since biomolecular assemblies in the cell are mostly exposed to varying  $\Pi$  while  $T$  is often constant. Therefore, it is of great importance to study bilayer structure and elastic properties such as bilayer bending rigidity  $\kappa$  or bilayer-bilayer interaction parameters as a function of osmotic pressure  $\Pi$ .

From the relation between the osmotic pressure  $\Pi$  and the lamellar spacing  $d$  the inter-bilayer interaction potentials can be determined. It is generally accepted that in charge neutral systems two main molecular interaction forces are dominant, in addition to the effective attractive interaction by osmotic pressure : a repulsive hydration potential  $f_{\text{hyd}}(d_w)$  and the attractive van der Waals potential  $f_{\text{vdW}}(d_w)$  so that the total interaction in  $\text{J/m}^2$  is given by  $f(d_w) = f_{\text{hyd}} + f_{\text{vdW}} + \Pi d_w$ , defining the equilibrium distance (water layer thickness)  $d_w$  as illustrated in Fig. 1 B). As discussed below, it is important to take the correct form for  $f_{\text{vdW}}$  as derived in [17], without the conventional half-space approximation. It can be argued that steric (Helfrich) repulsion forces have to be added to the molecular forces in a mean field approach. Here, however, we will assume that thermal fluctuations in thin films of relatively stiff phospholipids do not have a significant effect on the inter-bilayer interactions, in particular since the flat boundary suppresses long range fluctuations in the film. The paper is organized as follows : After this introduction, section 2 presents some experimental details while the statistical model and data analysis are presented

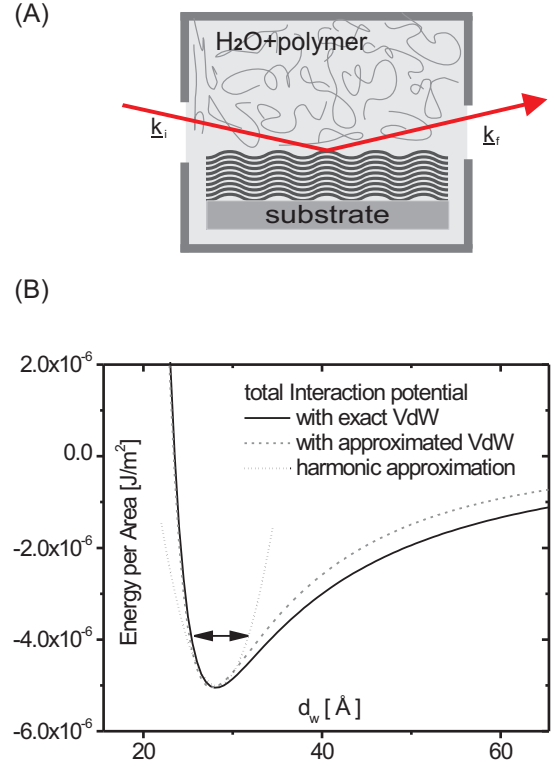


**Fig. 1.** A): Sketch of the experimental setup where a solid-supported membrane stack is hydrated in an aqueous polymer solution. Arrows indicate the incoming and scattered X-ray beams. B): Interaction potential with van der Waals contribution according to Fenzl [17] (solid line) and with general approximation (dashed). The (dotted) parabola illustrates the harmonic approximation to the potential which enters in the smectic elasticity theory. The arrow shows a typical fluctuation amplitude of a membrane inside a 16 bilayer stack.

in section 3. Section 4 presents the results, followed by a section on the interaction potentials and the conclusions in section 6.

## 2 Materials and Methods

### 2.1 Samples and Environment

Highly oriented oligo-membranes were prepared using the spin-coating method [14]. The uncharged lipid 1,2-dimyristoyl-sn-glycero-3-phosphocholine (DMPC) was bought from Avanti (Alabaster, AL, USA) and used without further purification. The lipid was dissolved in chloroform at a concentration of 10 mg/ml. An amount of 100  $\mu\text{l}$  of the solution was pipetted onto carefully cleaned silicon substrates of a size of  $15 \times 25 \text{ mm}^2$  cut from standard commercial silicon wafers. The substrate was then immediately accelerated to rotation (3000 rpm), using a spin-coater. After 30 seconds the samples were dry and

subsequently exposed to high vacuum to remove any remaining traces of solvent. The samples were then stored at 4 °C until the measurement. For the X-ray measurements the samples were hydrated in a stainless steel chamber [10] with kapton windows, which can be filled with water or with polymer solution to control the level of hydration by osmotic pressure, see the sketch in Fig. 1A. Temperature was controlled by an additional outer chamber at  $T = 40$  °C. The polymer polyethyleneglycol (PEG) of molar weight 20000 Da was bought from Fluka and used without further purification. PEG was dissolved in ultrapure water (Millipore, Billerica, Mass.) at the concentrations 1.5 %, 2.9 %, 3.6 %, 5.8 %, 9 %, 12.1 %, 14.2 % and 25 % (wt. percent). The corresponding osmotic pressure values were taken from the literature. The data was obtained from the web site of the Membrane Biophysics Laboratory at the Brock University in Canada (<http://aqueous.labs.brocku.ca/osfile.html>). The value for the osmotic pressure of PEG 20000 solutions is only available at 20 °C. At 40 °C, temperature at which the experiments were performed, the pressure can be expected to be somewhat lower. However, the temperature coefficient is small [16,19], and the corresponding discrepancy smaller than the error bars in Fig 6 below, which is used in the analysis of the interaction forces.

An important issue in our method of direct contact of the lamellar phase with the polymer solution is that of possible interpenetration of the multilamellar phase. Experiments on polymer containing lyotropic lamellar phases [20,21] have shown that polymers can enter the water layer in between charged bilayers even if the radius of gyration is larger than the water layer. However, in the present case of neutral polymer in neutral bilayers, the amount of polymer in between the lamellae is negligible. The experimental proof is given by (a) the density profile, which shows no deviation from the water density in between the bilayers, and (b) the force distance curve itself which shows no indication of such an effect.

## 2.2 X-ray experiment

The X-ray reflectivity measurements presented here were carried out at the bending magnet beamline D4 of HASYLAB/DESY in Hamburg, Germany. At D4, a single-reflection Si(111) monochromator was used to select a photon energy of 19.92 keV, after passing a Rh mirror to reduce higher harmonics. The chamber was mounted on the  $z$ -axis diffractometer, and the reflected beam was measured by a fast scintillation counter (Cyberstar, Oxford), using computer-controlled aluminum absorbers which attenuate the beam at small  $q_z$  to prevent detector saturation. Incident and exit beams were defined by a system of several motorized slits. The data is corrected for decreasing electron ring current and the diffuse contribution by subtraction of an offset scan. Finally, an illumination correction is performed. A typical measurement (reflectivity and offset scans) is shown in Figure 2, along with the corresponding Fresnel reflectivity. The inset shows a rocking

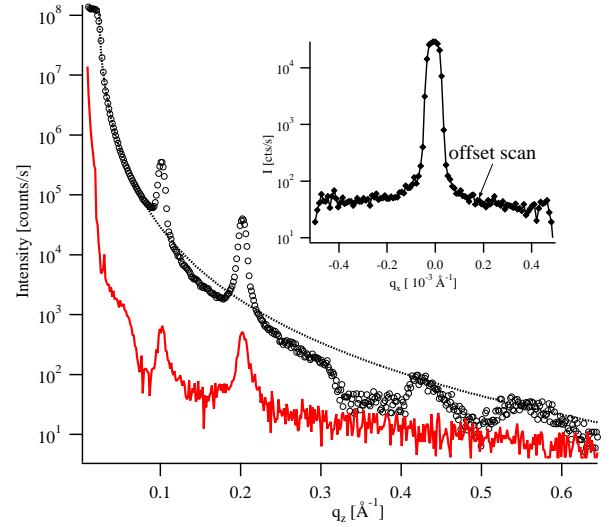


**Fig. 2.** Specular reflectivity scan (open symbols) and offset scan (red solid curve) for a sample immersed in pure water. The "true specular" contribution (see Appendix) is given by the difference of the two curves. In dotted line we also show the Fresnel reflectivity profile corresponding to the same critical angle  $q_c$ . Inset : Rocking scan at the position of the second Bragg peak. The arrow shows the  $q_x$  position of the offset scan.

scan on the second Bragg peak, illustrating the separation between "true specular" and diffuse components.

## 3 Model and data analysis

### 3.1 Reflectivity

In the semi-kinematic approximation the reflectivity of a structured interface can be expressed by the so-called master-formula of reflectivity [22] as :

$$R(q_z) = R_F(q_z) \cdot \left| \frac{1}{\rho_{12}} \int_{-\infty}^{\infty} \frac{d\rho(z)}{dz} e^{iq_z z} dz \right|^2, \quad (1)$$

where  $R_F$  denotes the Fresnel reflectivity of the sharp interface and  $\rho(z)$  is the intrinsic electron density profile, whereas  $\rho_{12}$  is the total step in electron density between the two adjoining media. The electron density profile of a solid-supported oligo-membrane stack, consisting of  $N$  membranes in water, can then be written as :

$$\rho(z) = \frac{\rho_{12}}{2} \operatorname{erfc}\left(\frac{z+d_0}{\sigma}\right) + \sum_{n=0}^{N-1} \rho_0(z - nd + u_n), \quad (2)$$

with  $\operatorname{erfc}(z)$  being the complementary error function and  $\sigma$  the rms substrate roughness.  $\rho_{12} = \rho_{\text{Si}} - \rho_{\text{H}_2\text{O}}$  is the difference in electron density between the substrate and water,  $d_0$  is the distance between the substrate and the midpoint of the first bilayer and  $\rho_0(z)$  is the electron density profile of one bilayer in the stack. Thermal membrane

fluctuations are considered in terms of the displacement function  $u_n = u(\mathbf{r}_{||}, z = nd)$  of the position of the  $n$ -th membrane from its average position  $z = nd$  along  $z$ . Replacing the electron density profile (2) into (1) and taking the ensemble average yields :

$$R(q_z) = R_F(q_z) \cdot \left[ e^{-q_z^2 \sigma^2} - 2i \cdot e^{-\frac{q_z^2 \sigma^2}{2}} \sum_{n=0}^{N-1} f(n) \left( Ff(q_z) \cdot \sin(q_z(d_0 + nd)) e^{-\frac{q_z^2}{2} \langle u_n^2 \rangle} \right) + |Ff(q_z)|^2 \cdot \sum_{m,n=0}^{N-1} f(n)f(m) e^{-iq_z d(m-n)} e^{-\frac{q_z^2}{2} (\langle u_m^2 \rangle + \langle u_n^2 \rangle)} \right].$$

The first summand represents the reflectivity of the substrate. The second is a cross-term and represents interference effects between the substrate and the membrane stack. The third summand is the product of the form factor  $|Ff(q_z)|^2$  containing the structural information about one bilayer in the stack, and the structure factor, representing the periodic structure in the stack. The fluctuations are described by the correlation function  $\langle u_n u_m \rangle$ . In specular reflectivity only the self-correlation function  $\langle u_n^2 \rangle$  is important (see Appendix).

### 3.2 Correlation Function

The self-correlation function of the membrane fluctuations can be calculated from linear smectic elasticity theory based on a continuous model [23]. The complete theory and calculations are described in [24]. Here only the essentials, which are important for specular reflectivity shall be given. The linearized free energy can be written as a function of the displacement  $u(\mathbf{r}_{||}, z)$  as :

$$F = \frac{1}{2} \int_V d\mathbf{r} \left[ B \left( \frac{\partial u(\mathbf{r}_{||}, z)}{\partial z} \right)^2 + K (\Delta_{||} u(\mathbf{r}_{||}, z))^2 \right], \quad (3)$$

with  $K = \kappa/d$  the bending modulus and  $B$  the compression modulus in the stack. We neglect the surface tension between the lipid stack and the solvent. The discrete structure of the stack consisting of  $N$  bilayers is taken into account by expanding  $u$  over  $N$  independent modes. Also, we are only interested in the fluctuation amplitude at the position of the bilayer midpoints, denoted by  $u_n = u(z = nd)$  for the  $n$ -th bilayer. From the equipartition theorem one can calculate the correlation function of the membrane fluctuations  $\langle u_n^2 \rangle$ , which reads :

$$\langle u_n^2 \rangle = \eta \left( \frac{d}{\pi} \right)^2 \sum_{j=1}^N \frac{1}{2j-1} \sin^2 \left( \frac{2j-1}{2} \pi \frac{n}{N} \right) \quad (4)$$

with the conventional Caillé factor  $\eta = \frac{\pi}{2d^2} \frac{k_B T}{\sqrt{BK}}$ . Figure 5A shows the function for a 16 membrane stack with a typical  $\eta$  value for DMPC membranes at partial hydration. In contrast to oligo-membranes which are partially

hydrated from water vapor, oligo-membranes immersed in excess water or polymer solution exhibit defects which result in decreasing layer coverage with increasing distance from the substrate. This effect is evidenced experimentally by the suppression of thickness oscillations (Kiessig fringes) in the reflectivity curves. Thickness oscillations are typically observed in vapor-hydrated samples but are significantly reduced or suppressed in samples immersed in aqueous solution [14,25]. In the model we take this effect into account by multiplying the contribution of each membrane in the structure-factor with an empirical coverage-factor  $f(n) = [1 - (n/N)^\alpha]^2$ , where  $\alpha$  parameterizes the decaying density due to decreasing coverage. A typical experimental value is  $\alpha \approx 1.7$ . Note that both  $\alpha$  and the number of bilayers  $N$  are fit parameters.

Since the form factor  $|Ff(q_z)|^2$  of the membranes consists of the squared Fourier transform of the  $z$ -derivative of the electron density profile of the membrane, it is convenient to express the profile in terms of normalized Fourier coefficients [15]

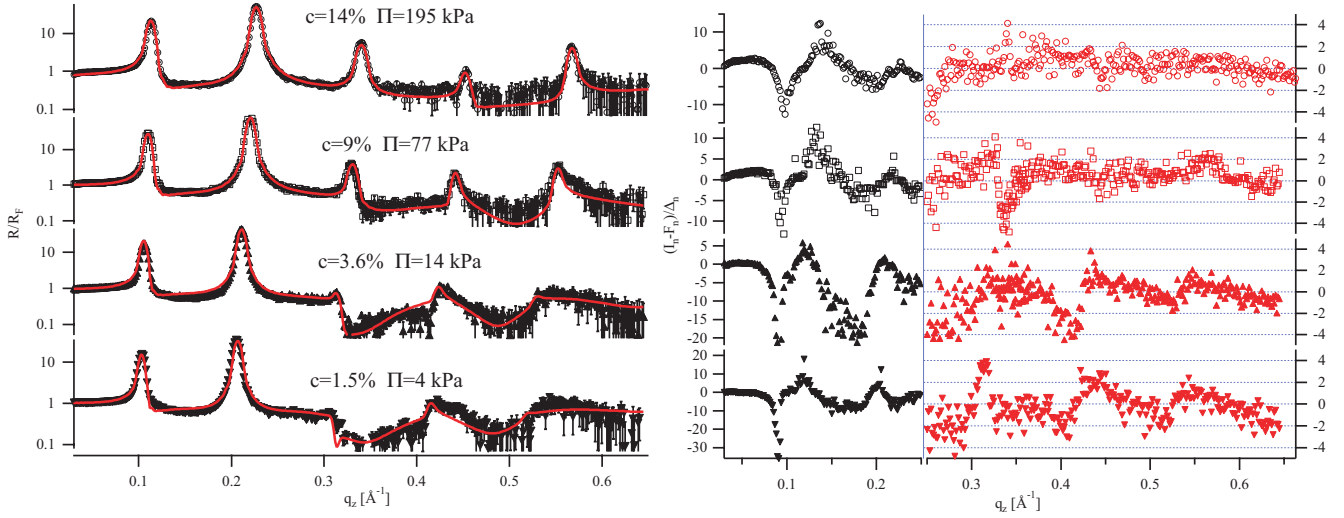
$$\rho(z) = \sum_{m=1}^{N_0} f_m \cdot \cos \left( \frac{2\pi m z}{d} \right) \cdot \rho_{12} + \bar{\rho} - \rho_w,$$

with  $\bar{\rho}$  being the average electron density of the membrane stack and  $\rho_w$  the electron density of water. For DMPC,  $\bar{\rho} = 0.3397 \text{ e}^-/\text{\AA}^3$  [4], very close to  $\rho_w = 0.332 \text{ e}^-/\text{\AA}^3$ , so that  $|Ff(0)| \simeq 0$ .

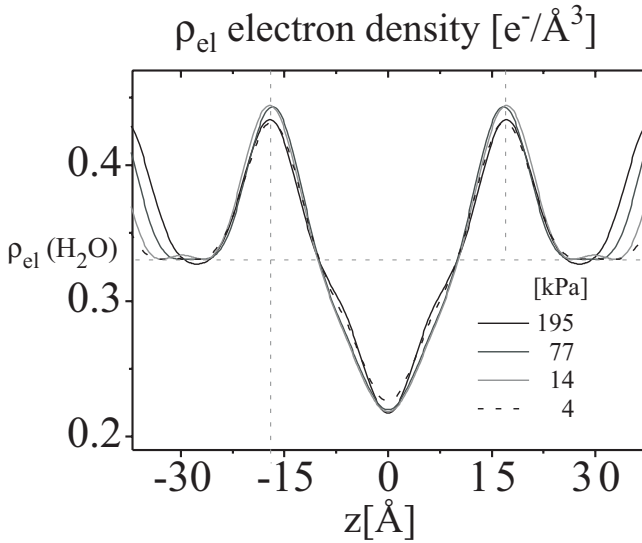
## 4 Reflectivity results

Figure 3 shows the reflectivity measurements (symbols) of 16 DMPC membranes on silicon substrates at four (out of nine measured) different osmotic pressures. The curves have been stacked vertically for clarity, with increasing pressure from 4 kPa (bottom) to 195 kPa (top). The continuous lines are simulations based on the model described above with the corresponding electron density profiles shown in Figure 4A. The reflectivity spectra presented in Figure 3 were each scaled by the corresponding Fresnel reflectivity. The error bars in the intensity at point  $n$ ,  $\Delta I_n$ , are estimated considering Poissonian statistics (both for the raw reflectivity and for the offset scan). The error bar in the  $q_z$  direction is taken as  $\Delta q_n = \Delta q = 5 \times 10^{-4} \text{\AA}^{-1}$ , corresponding roughly to the symbol size, and is given by the estimated precision in sample alignment.

From the electron density profiles one can see that the increase of periodicity  $d$  with decreasing pressure is mainly due to changes in the water layer thickness, while the bilayer structure is essentially invariant over the range in  $\Pi$  studied, with a headgroup spacing (distance between the two maxima in the electron density profile)  $d_{HH} = 34 \pm 0.5 \text{\AA}$ , in good agreement with the value of  $34.4 \text{\AA}$  given by Petrache *et al.* [4]. The simulations match the measured reflectivity curves not only at the position of the Bragg peaks, but in the whole continuous  $q$ -range of the measurement. At lower osmotic pressure  $\Pi$  the higher



**Fig. 3.** Left : Symbols : measured reflectivity curves of 16 DMPC membranes on silicon substrates under different osmotic pressures, normalized by the corresponding Fresnel reflectivity. Solid lines : show full  $q$ -range simulations using the described model, with the density profiles given in Figure 4. The polymer concentration and the osmotic pressure are specified for each curve. Right : Residues of the reflectivity data, normalized by the estimated standard deviation (see text for details). The graph is horizontally split into two panels, with different  $y$  axes : Below  $0.25 \text{ \AA}^{-1}$ , the large discrepancies correspond to systematic errors, while for  $q_z > 0.25 \text{ \AA}^{-1}$  the residues are more randomly distributed and their scaled amplitude is below 5.



**Fig. 4.** Electronic density profile of the bilayer, as a function of the applied osmotic pressure  $\Pi$ .

order peaks are suppressed due to increased thermal fluctuations, as quantified by the above model. As an illustration, Fig. 5A shows the increase in the fluctuation amplitude as a function of the membrane index for a 16 bilayer sample.

As discussed above, the relevant parameters for the reflectivity curves are the mean squared fluctuation amplitudes  $\langle u_n^2 \rangle$ , which give access to the Caillé parameter  $\eta$ . In order to compare our data to the bulk results [4] we then compute the interbilayer spacing fluctuation am-

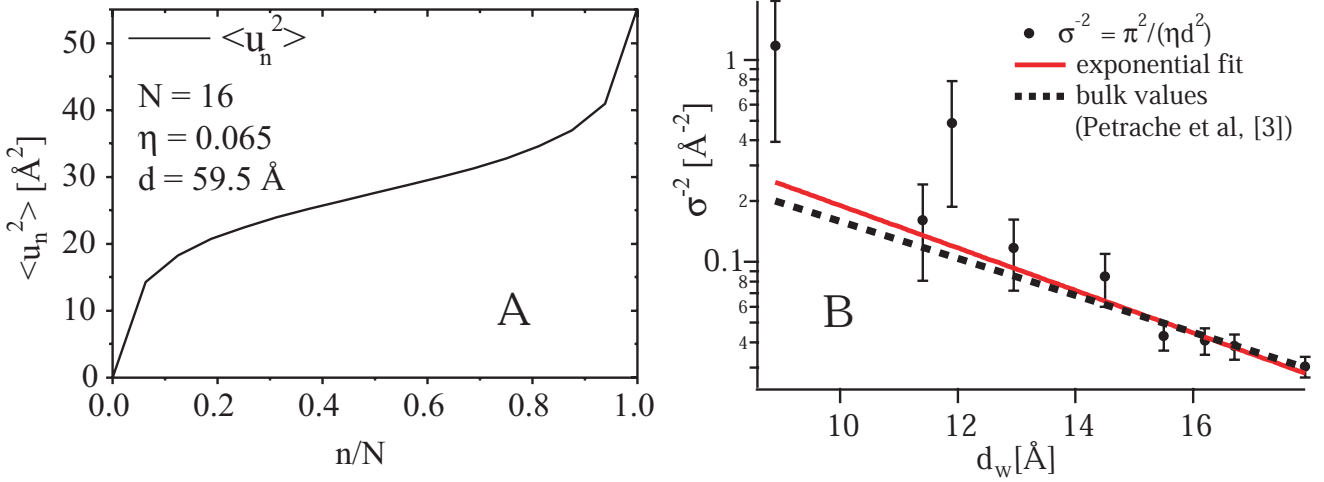
plitude  $\sigma^2 = \langle (u_n - u_{n-1})^2 \rangle = \eta \frac{d^2}{\pi^2}$ . Soft confinement theories predict an exponential dependence [4] of parameter  $\sigma^2$  with the interbilayer distance, which can be taken as the thickness of the water layer, given by  $d_w = d - d_B$ , where  $d_B = 44 \text{ \AA}$  is the thickness of the DMPC bilayer [4].

Fig. 5B shows the reciprocal of the fluctuation amplitudes as a function of the water spacing  $\sigma^{-2}(d_w)$ , along with a fit to an exponential decay (solid line). The data points can be fitted to an exponential function  $\sigma^{-2} \propto \exp(-d_w/\lambda_\Pi)$ , with a decay length  $\lambda_\Pi = 4.1 \pm 0.9 \text{ \AA}$ , comparable to the results of the bulk study, which also reports exponential behaviour (shown as a dashed line) with  $\lambda_\Pi = 5.1 \text{ \AA}$  [3].

The lamellar periodicity  $d$  was measured for all values of the osmotic pressure  $\Pi$ , up to 870 kPa. We show  $\Pi(d)$  in Figure 6 (diamonds). For comparison, we also plotted the fit by Petrache *et al.* of the bulk data, Figure 7, upper panel in their paper [4] (dashed line). They performed the measurements at  $30^\circ\text{C}$  and obtain  $d_0 = d(\Pi = 0) = 62.7 \text{ \AA}$ , while our experiments, performed at  $40^\circ\text{C}$ , yield  $d_0 = 61.9 \text{ \AA}$ . This deviation is in agreement with recent data of  $d_0(T)$  for DMPC [26]. A quick test can be performed by shifting their curve by  $0.8 \text{ \AA}$  to lower  $d$  values (solid line). The agreement is good, but a more detailed analysis is obviously needed for a meaningful comparison.

## 5 Interaction potentials

We saw above that our data can be brought to agreement with the bulk equation of state  $\Pi(d)$  by the  $0.8 \text{ \AA}$  shift, which can be attributed to the temperature difference. Consequently, the interaction potentials derived from the



**Fig. 5.** A) Amplitude of the bilayer position fluctuations  $\langle u_n^2 \rangle$  in a solid-supported membrane stack consisting of 16 DMPC membranes at partial hydration, controlled by an osmotic pressure of 4 kPa (used for the model in Fig. 3, bottom). B) Reciprocal of the squared fluctuation amplitudes  $\sigma^{-2}(d) = \pi^2/(\eta d^2)$ , as determined from the reflectivity fits, and exponential fit (solid line). Also shown is the exponential fit to the bulk data of Petrache *et al.* [4]. For clarity, their experimental data points are not shown.

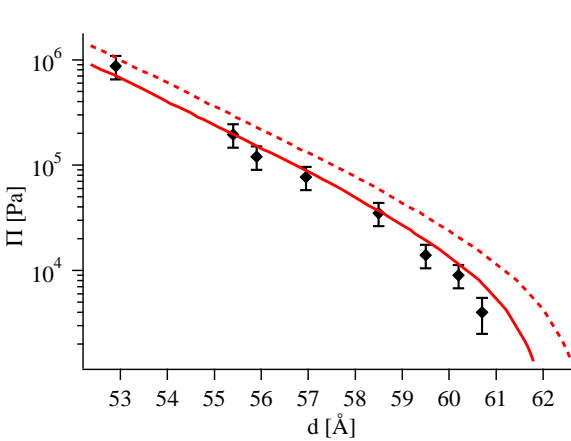


**Fig. 6.** Osmotic pressure  $\Pi$  as a function of the lamellar  $d$  spacing. Diamonds : experimental data points. Dashed line : Fit to the bulk data of Petrache *et al.* [4]. For clarity, their experimental data points are not shown. Solid line: same curve shifted to lower  $d$  values to account for the effect of temperature (see text for details).

bulk and the present data will also be identical or at least similar. However, the choice of the functional forms for the potentials, the geometric partitioning of the bilayer to calculate the van der Waals part and the choice of the bending rigidity  $\kappa$  can all be debated. We therefore first give a brief discussion of the different interaction potentials used for neutral lipid membranes, and then present results based on modelling the equation of state  $\Pi(d)$ .

The hydration potential is usually empirically described by an exponential function of the water layer thickness  $d_w$  [27] :

$$f_{\text{hyd}}(d_w) = H_0 \exp(-d_w/\lambda) , \quad (5)$$

with a prefactor of the order of  $H_0 = k_B T / \text{\AA}^2$  and a decay length on the order of a few Angstroms  $\lambda = 1 - 2 \text{ \AA}$ . For the van der Waals potential, Petrache *et al.* [3], used the following expression and geometric convention:

$$V_{\text{vdW}}(d_w) = \frac{H_{\text{vdW}}}{16\pi} \left[ \frac{1}{d_w^2} - \frac{2}{(d_w + d_B)^2} + \frac{1}{(d_w + 2d_B)^2} \right] , \quad (6)$$

where  $d_w$  is the water layer and  $d_B = d - d_w$  the bilayer thickness. The expression should be regarded as an approximation to the result of a more detailed treatment, as discussed by Fenzl [17]. Accordingly, the potential should be calculated from

$$F_{\text{vdW}}(d_h, T) = 0.9 \frac{k_B T}{8\pi d_h^2} \sum_{n=0}^{\infty} \int_{r_n}^{\infty} dx x \quad (7)$$

$$\ln \left[ 1 - \left( \frac{\Delta_n (1 - \exp(-ax/d_h))}{1 - \Delta_n^2 \exp(-ax/d_h)} \right)^2 \exp(-x) \right] ,$$

where  $d_h$  is again the thickness of the hydrophilic layers consisting of the water layer and the headgroups and  $\Delta_n = (\epsilon_{\text{H}_2\text{O}}(\omega_n) - \epsilon_{\text{CH}_2}(\omega_n)) / (\epsilon_{\text{H}_2\text{O}}(\omega_n) + \epsilon_{\text{CH}_2}(\omega_n))$  is a function of the frequency-dependent dielectric constants of hydrocarbon and water. The prime symbol ' indicates that the static term ( $n = 0$ ) has to be multiplied by 1/2. The calculation is somewhat involved, however Fenzl has shown that a frequently used approximation of Eqs. 6 is valid for the dispersion term, but not for the static term which dominates under salt-free conditions. Moreover, Podgornik and coworkers have shown that nonpairwise additive contributions to the van der Waals interaction play a significant role in multilayers at large swelling [28]. However, for the present parameters, the above treatment should be sufficient.

Apart from the molecular forces discussed above, steric forces resulting from membrane bending elasticity should

be included, as first introduced by Helfrich [29]. Accordingly, a repulsive undulation force arises

$$f_{U1} = 0.42 \frac{(k_B T)^2}{\kappa d_w^2}, \quad (8)$$

which cannot, however, be simply added to the molecular forces. Instead, steric forces must be treated by field theoretical approaches which go beyond the mean field approximation [1], or by self-consistent models [30], but which to date have not been combined with realistic molecular potentials in multilamellar stacks. Facing these complications, Petrache and coworkers [3] have pointed out that the measured rms-fluctuation of the next neighbor distance  $\sigma = \sqrt{\eta}d/\pi$  can be used to experimentally determine the fluctuation pressure  $P_{fluct}$ , which they then added to the pressure calculated from the molecular potentials to fit their data  $\Pi(d) = P_{mol} + P_{fluct}$ . Obviously, this approach avoids the problematic identification of the thermodynamic compression modulus to the bulk modulus  $B$  as defined in the Caillé model, but still assumes that the total pressure can be written as a sum, which may strictly only be true in mean field approximation. The advantage of the approach is that it makes clever use of the experimental information from either of the interconnected functions  $B(d)$ ,  $\eta(d)$ , or  $\sigma(d)$  to compute the pressure. According to [3]

$$P_{fluct} = -\frac{(4k_B T)^2}{(8\pi)^2} \frac{1}{\kappa} \frac{d\sigma^{-2}}{d(d_w)}. \quad (9)$$

Fig. 5 shows the measured parameter the inverse of the fluctuation amplitudes  $\sigma^{-2}(d)$ , along with a fit to an exponential decay (solid line). The data points can be fitted to an exponential function  $2.14 \exp(-d_w/4.17) \text{ \AA}^{-2}$ . Subtracting the corresponding fluctuation pressure  $P_{fluct}$  obtained by differentiation according to Eq. 9 for a given parameter  $\kappa$  from  $\Pi(d)$ , the molecular interactions (hydration and van der Waals interactions) can then be modelled and compared to the data, as shown below in Fig. 7.

Below we give results for two different approaches in the data analysis. The first approach is described in detail in [31]. It is based on the assumption that the periodicity  $d$  is dominated by the molecular forces, and that steric forces are comparatively small for relatively stiff phospholipid membranes.

First approach: The calculation of the van der Waals interaction was based on equation (7) for the static contribution. The static part for  $n = 0$  was numerically integrated between 0 and 100. For water  $\epsilon_{H_2O}(0) = 80$  and for hydrocarbon (tetradecane)  $\epsilon_{CH_2}(0) = 2$  was taken. For the dispersion term a hydrophobic bilayer thickness  $26 \text{ \AA}$  and a Hamaker constant  $H_{dis} = 0.297$  was used. The latter value has been chosen to approximate (7), evaluated for dispersion relations  $\epsilon_{H_2O}(\omega)$  and  $\epsilon_{CH_2}(\omega)$  which have been parameterized by oscillator models as in [17]. Note that in this approach there is no free parameter for the vdW interaction. Figure 1 B shows the total interaction potential (solid line) with separately calculated static

and dispersion terms as described above. A calculation based only on Eq. 6 (with adjusted Hamaker constant) is shown for comparison (dashed curve). The parameters of the hydration interaction which were then freely adjusted were  $H_0 = 4.8 k_B T / \text{\AA}^2$  and  $\lambda = 1.88 \text{ \AA}$ . The 10% reduction from the fixed values in [17] in the van der Waals term for equation (7) may be attributed to the fact that Helfrich repulsive forces have not been included in the force balance. At the same time, it is interesting to note the value obtained for  $\kappa$  in this approach. To estimate  $\kappa$  we note that the Caillé parameter  $\eta = \frac{\pi^2}{2d^2} \frac{k_B T}{\sqrt{B\kappa/d}}$  has been determined

from the full  $q$ -range fits to the reflectivity curves at different pressures. As the compression modulus  $B(d) = \partial\Pi/\partial d$  has been independently determined by numerical derivation of the measured  $\Pi(d)$  curve, one can now estimate the bending modulus  $\kappa$  from the experimental values of  $\eta(d)$ . The best agreement was obtained for  $\kappa = 23.2 \pm 2.5 k_B T$ . Within these uncertainties  $\kappa \simeq 23 k_B T$  compares quite well with the value of  $\kappa = 19 k_B T$  at  $30^\circ\text{C}$  determined from bulk suspensions of DMPC by Petrache *et al.* [3]. Note however that another study employing full  $q$ -range fits and osmotic pressure variation reports  $\kappa = 11.5 k_B T$  [32], again at full hydration and comparable  $T$ . Finally, thermal diffuse scattering analysis points to significantly smaller values  $\kappa = 7 k_B T$  [33]. Note that the determination of  $\kappa$  from the osmotic pressure series is based on a problematic assumption, i.e. that the identification of the bulk modulus  $B$  as defined in the Caillé model and the thermodynamic compression modulus is correct. More details on the data analysis following this approach based on molecular interactions only are given in [31].

In the second approach we followed exactly the procedure given by [3]. First, the fluctuation pressure is subtracted from  $P(d)$ , and then the resulting bare pressure is modelled in terms of the molecular interactions. However, the calculation of the fluctuation pressure according to equation 9 needs the bending rigidity  $\kappa$  as an additional parameter. To illustrate the range of parameter variability, we present a comparison of two different choices of parameters: (a) all parameters and functions are kept as close as possible to those used in [3], in particular keeping  $\kappa = 18.5 k_B T$  fixed. The corresponding values for  $H_0 = 0.020 \text{ J/m}^2$  and  $H_{vdW} = 4.91 \cdot 10^{-21} \text{ J}$  are practically identical to the values in [3], showing that the same approach can explain both bulk and thin film data. The same treatment has then been carried out for a different choice of  $\kappa = 8 k_B T$ . Again the simulations can be brought into agreement with the data, but only for a different set of parameters  $H_0 = 0.028 \text{ J/m}^2$  and  $H_{vdW} = 1.1 \cdot 10^{-20} \text{ J}$ . Thus values at the lower and upper range of the  $\kappa$  values reported in the literature both lead to reasonable agreement, indicating that extra information from other experiments is needed to unambiguously determine the potentials. The potentials are shown for the two cases, and can be compared also to the potential in Fig. 1(b), derived from the data analysis under the assumption that the fluctuation repulsion is negligible.

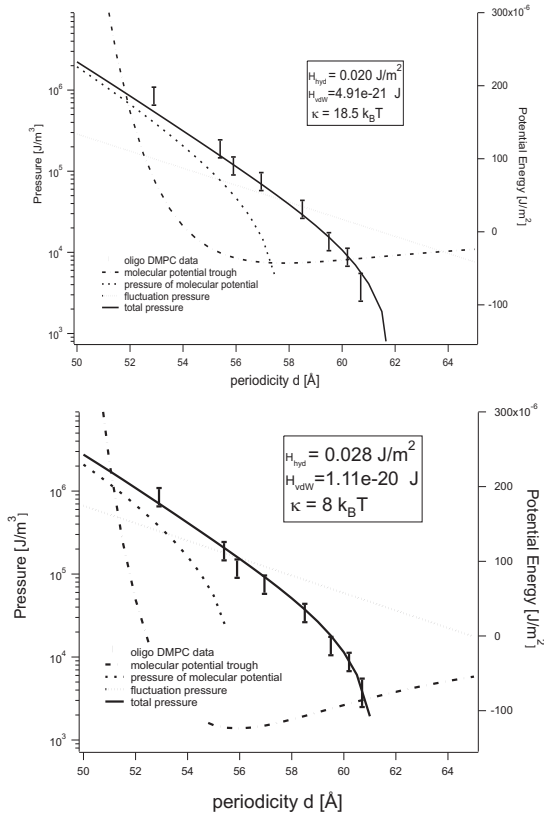


**Fig. 7.** Osmotic pressure  $\Pi$  as a function of lamellar periodicity  $d$  (same data as in Fig. 5(A)). The simulations have been carried out following the approach of [3] for (a) fixed  $\kappa = 18.5 k_B T$  and (b)  $\kappa = 8 k_B T$ . The parameters of the hydration interaction  $H_0$  (Eq. 5) and the Hamaker constant  $H_{vdW}$  (Eq. 6) are varied to match the data. The simulations in (a) and (b) show the total pressure (solid line), the fluctuation pressure  $P_{fluct}$  (dotted line), the pressure corresponding to the molecular potential (dashed line), and the potential trough corresponding to the molecular forces (dash-dotted line). The fluctuation pressure as determined from Eq. 9 and the data in Fig. 5 was added to the pressure stemming from the molecular forces.

## 6 Discussion and Conclusions

In conclusion, we have presented an osmotic pressure experiment on thin solid-supported lipid multilayers (oligo-membranes). The x-ray reflectivity has been measured and modelled over the full  $q_z$ -range up to  $0.7 \text{ \AA}^{-1}$ . From this analysis fluctuation and structural parameters can be obtained, similar to the lineshape analysis of bulk suspensions [3,5]. Solid-supported oligo-membranes offer some advantages both over thick multilamellar films and the bulk counterpart. Long range thermal fluctuations are not as strong as for bulk samples, and the scattering can be probed up to higher momentum transfer. Owing to the

smaller number of bilayers, destructive interference in-between the Bragg peaks is not quite as strong as in thick stacks of several hundred bilayers. To achieve satisfactory fits, two important effects were taken into account: (i) the static defects leading to a decreasing coverage of the bilayers from the substrate to the top of the film, and (ii) the thermal fluctuations of the bilayers subject to the boundary condition of a flat substrate [24]. While (i) most likely reflects non-equilibrium aspects of sample deposition and/or equilibrium wetting properties (not further analyzed here), (ii) is exploited to deduce interaction parameters in the framework of linear smectic theory. The curve  $B(d)$  derived from the osmotic pressure series  $\Pi(d)$  is subsequently modelled based on different interaction potentials. However, this modelling cannot be carried out without assumptions or additional theoretic arguments.

In the data analysis, we have presented two entirely different approaches to illustrate how the determination of interaction forces depends on the specific assumptions, theoretical arguments, or extra information taken from other experiments. The first approach builds upon the rather strong assumption that steric forces are negligible and that the derivative of the equation of state  $\partial \Pi(d)/\partial d$  can be identified with the modulus  $B(d)$  which controls the thermal fluctuations. It then yields the parameters of the hydration force necessary to balance the van der Waals attraction at each given osmotic pressure. This approach also gives a value for the bending constant from simultaneous inspection of  $B(d)$  and  $\eta(d)$ . However, the resulting  $\kappa \simeq 23 k_B T$ , is probably an overestimation. The rather large value may point to the fact that  $B$  is underestimated by the contribution of only the bare potentials. Adding a fluctuation pressure would tend to increase  $B$  and thus decrease  $\kappa = K d$ . Note that this determination of  $\kappa$  is conceptually very different from a more direct assessment of  $\kappa$ , e.g. from the measurement of diffuse scattering.

The second approach includes the steric Helfrich undulation forces. This contribution is a subtle issue for the following reasons: (a) it has been shown by Lipowsky and coworkers that the Helfrich term cannot be simply added to the molecular forces. If one nevertheless uses a mean field approach, (b) the functional form to be used as well as the numerical prefactor are still under debate [34]. Therefore, we have followed an idea of Petrache et al. [3], who have carried out an osmotic pressure study on DMPC, which is the bulk analogue of the present work. Calculating the partition function within the linear smectic elasticity model, they have derived an expression for the fluctuation pressure as a function of a measurable quantity, namely the derivative of the fluctuation amplitudes, see Eq. 5. In a mean field treatment, they add this pressure to the bare pressure calculated from the interaction potentials and fit the sum to the measured curve  $\Pi(d)$ . In this step, an assumption of  $\kappa$  has to be made, e.g. from other experimental data. This approach has been carried out for two choices of  $\kappa$ , see Fig. 7.

We point out, however, that the questions related to the interaction potentials arise only on a secondary level,

where structural results ( $d$  and  $\sigma$ ) are interpreted and transformed to elasticity and interaction parameters. On the primary level that the structural results presented here, *i.e.*  $\Pi(d)$ ,  $\rho(z, \Pi)$  and  $\langle u_n^2 \rangle(d)$  are well supported by the curves and fits shown here. The second level is necessarily model-dependent. We have presented two alternative approaches to illustrate the relation and interdependencies of different assumptions and results. It may be justified to conclude that the second approach as proposed and used by [3] is more appropriate, since steric repulsion is known to be important. However, the choice of the van der Waals expression may have to be improved to a more accurate form, and the choice of  $\kappa$  is also an important issue. Unfortunately, the second approach also relies on the validity of a mean field approximation. This simplification could be eliminated in the future by generalization of a recent self-consistent calculation for bilayer fluctuations and interactions [30] to the case of several membranes or by use of the approach developed in [35]. Furthermore, non-linear effects due to the asymmetry of the potential could also be included by more general models [36, 35] and/or numeric simulations. To elucidate the validity of the linearized model *a posteriori*, the rms-deviation  $\sqrt{\langle (u_n - u_{n+1})^2 \rangle}$  between neighboring membranes can be compared to the width of the inter-bilayer potential well, see Figure 1 (B). For  $N = 16$  and  $\eta = 0.08$  (full hydration) the bilayers in the center of the stack already exhibit considerable next-neighbor distance fluctuations in the range of 4 – 5 Å, when compared to the water layer thickness. Thus the errors made in the simplifying assumptions are probably not negligible. We note, however, that at least under high osmotic pressure, where fluctuations are small, both the mean field approach and the harmonic approximation for the potential should hold.

## Appendix

In this appendix, we give a sketch of the derivation of our formula (3.1) for the reflectivity, insisting upon the separation between the specular and diffuse components. This is a classical result and a more detailed derivation can be found in references [37] (equation 2.28) and [22] (subsection 3.8.3) for the case of single interfaces and in [38] (section 3) for multiple interfaces.

It is well known that bulk lamellar phases exhibit the Landau-Peierls instability, leading to a characteristic power-law variation of the scattered signal [6]. In such a system the fluctuation amplitude  $\langle u_n^2 \rangle$  diverges. It is then more appropriate to use the correlation of the height difference, which remains finite for all finite values of  $r$ :

$$g_{mn}(\mathbf{r}_{\parallel}) = \langle (u_m(\mathbf{r}_{\parallel}) - u_n(\mathbf{0}))^2 \rangle \quad (10)$$

$$= \langle u_m^2 \rangle + \langle u_n^2 \rangle - 2\langle u_m(\mathbf{r}_{\parallel})u_n(\mathbf{0}) \rangle$$

It is then easy to show [37, 38] that the structure factor of the lamellar stack (without taking into account the

substrate contribution, so only the third term in Eq. (3.1) is described) reads :

$$S(\mathbf{q}) = \sum_{m,n} e^{-iq_z d(m-n)} \int d\mathbf{r}_{\parallel} e^{-i\mathbf{q}_{\parallel} \mathbf{r}_{\parallel}} e^{-\frac{1}{2}q_z^2 g_{mn}(r)}. \quad (11)$$

where  $r = |\mathbf{r}_{\parallel}|$ , assuming that the fluctuations are isotropic in the membrane plane. For bulk systems,  $\lim_{r \rightarrow \infty} g_{mn}(r) = \infty$ , so that  $\lim_{r \rightarrow \infty} \exp[-\frac{1}{2}q_z^2 g_{mn}(r)] = 0$  and the Fourier transform with respect to  $\mathbf{r}_{\parallel}$  in formula (11) yields a "smooth" function  $S(\mathbf{q}_{\parallel})$  at fixed  $q_z$ . If, however,  $g_{mn}(r)$  does not diverge for  $r \rightarrow \infty$ , the function  $\exp[-\frac{1}{2}q_z^2 g_{mn}(r)]$  now has a constant background, at a value of  $\exp[-\frac{1}{2}q_z^2 g_{mn}(\infty)] = \exp[-\frac{1}{2}q_z^2 (\langle u_m^2 \rangle + \langle u_n^2 \rangle)]$ , quantifying the "remanent order" in the system. Its Fourier transform is a Dirac delta function  $\delta(\mathbf{q}_{\parallel})$  (in practice, its width is given by a combination of resolution effects, beam coherence and system size). This term is sometimes called the "true specular component", because the smooth function discussed above (the "diffuse" component) also contributes to the specular signal  $S(\mathbf{q}_{\parallel} = \mathbf{0}, q_z)$ . However, as the diffuse scattering varies over a much larger  $\mathbf{q}_{\parallel}$  range, it can be accounted for in the first approximation by an offset scan taken close enough to the specular sharp peak (see figure 2). Finally, we can write :

$$S_{\text{spec}}(\mathbf{q}_{\parallel} = \mathbf{0}, q_z) = \sum_{m,n} e^{-iq_z d(m-n)} e^{-\frac{1}{2}q_z^2 (\langle u_m^2 \rangle + \langle u_n^2 \rangle)} \quad (12)$$

which is the form employed in equation (3.1). It is noteworthy that this "true specular" contribution is distinct in nature from the signal measured in SAXS experiments on powder samples, where only the diffuse signal persists.

Guillaume Brotons is acknowledged for helpful discussions on the osmotic stress technique. D. C. has been supported by a Marie Curie Fellowship of the European Community programme *Improving the Human Research Potential* under contract number HPMF-CT-2002-01903.

## References

1. R. Lipowsky. Generic interactions of flexible membranes. In R. Lipowsky and E. Sackmann, editors, *Handbook of Biological Physics*, volume 1, pages 521–602. Elsevier Science, Amsterdam, 1995.
2. C.R. Safinya, E. B. Sirota, D. Roux, and G.S. Smith. *Phys. Rev. Lett.*, 62:1134–1137, 1989.
3. H.I. Petrache, N. Gouliarov, S. Tristram-Nagle, R. Zhang, R. M. Suter, and J.F. Nagle. *Phys. Rev. E*, 57:7014–7024, 1998.
4. H. Petrache, S. Tristram-Nagle, and J.F. Nagle. *Chem. Phys. Lipids*, 95:83, 1998.
5. G. Pabst, M. Rappolt, H. Amenitsch, and P. Laggner. *Phys. Rev. E*, 62:4000–4009, 2000.
6. A. Caillé. *C. R. Acad. Sci. Paris, Sér. B*, 274:891, 1972.

7. R. Zhang, R. M. Suter, and J. F. Nagle. *Phys. Rev. E*, 50:5047–5060, 1994.
8. G.S. Smith, E.B. Sirota, C.R. Safinya, and N.A. Clark. *Phys. Rev. Lett.*, 60:813, 1988.
9. Y. Lyatskaya, Y. Liu, S. Tristram-Nagle, J. Katsaras, and J.F. Nagle. *Phys. Rev. E*, 63:011907, 2000.
10. M. Vogel, C. Münster, W. Fenzl, and T. Salditt. *Phys Rev. Lett.*, 84:390–393, 2000.
11. T. Salditt, M. Vogel, and W. Fenzl. *Phys Rev. Lett.*, 90:178101, 2003.
12. Y. Liu and J.F. Nagle. *Phys. Rev. E*, 69:040901, 2004.
13. G. Fragneto, T. Charitat, F. Graner, K. Mecke, L. Perino-Gallice, and E. Bellet-Amalric. *Europhys. Lett.*, 53:100–106, 2001.
14. U. Mennicke and T. Salditt. *Langmuir*, 18:8172–8177, 2002.
15. T. Salditt, C. Li, A. Spaar, and U Mennicke. *Eur. Phys J. E.*, 7:105–116, 2002.
16. V.A. Parsegian, R.P. Rand, N.L. Fuller, and D.C. Rau. Osmotic stress for the direct measurement of intermolecular forces. In L. Packer, editor, *Methods in Enzymology*, volume 127. Academic Press, New York, 1986.
17. W. Fenzl. *Z. Phys. B*, 97:333–336, 1995.
18. G. Brotons, T. Salditt, M. Dubois, and Th. Zemb. *Langmuir*, 19:8235–8244, 2003.
19. C. Stanley and H. Strey. *Macromolecules*, 36:6888, 2003.
20. C. Ligoure, G. Bouglet, G. Porte, and O. Diat. *J. Phys. II*, 7:473, 1997.
21. F. Castro-Roman, G. Porte, and C. Ligoure. *Phys. Rev. Lett.*, 82:109, 1999.
22. J. Als-Nielsen and D. McMorrow. *Elements of Modern X-Ray Physics*. Wiley, Chichester, 2001.
23. A. Poniewierski and R. Holyst. *Phys. Rev. B*, 47:9840–9843, 1993.
24. D. Constantin, U. Mennicke, C. Li, and T. Salditt. *Eur. Phys. J. E*, 12:283–290, 2003.
25. L. Perino-Gallice, G. Fragneto, U. Mennicke, T. Salditt, and F. Rieutord. *Eur. Phys. J. E*, 8:275–282, 2002.
26. G. Pabst, H. Amenitsch, P. Kharakoz, P. Laggner, and M. Rappolt. *Phys. Rev. E*, 70:021908, 2004.
27. R.P. Rand. *Annu. Rev. Biophys. Bioeng.*, 10:227, 1981.
28. R. Podgornik, R. H. French, and V. A. Parsegian. *J. Chem. Phys.*, 124:044709, 2006.
29. W. Helfrich. *Z. Naturforsch.*, 28c:693, 1973.
30. K.R. Mecke, T. Charitat, and F. Graner. *Langmuir*, 19:2080–2087, 2003.
31. U. Mennicke. *Structure and Fluctuations of Solid-Supported Phospholipid Membranes (in German)*. PhD thesis, Göttingen University, 2003.
32. G. Pabst, J. Katsaras, V. A. Raghunathan, and M. Rappolt. *Langmuir*, 19:1716–1722, 2003.
33. T. Salditt, M. Vogel, and W. Fenzl. *Phys Rev. Lett.*, 93:169903, 2004.
34. T. Schilling, O. Theissen, and G. Gompper. *Eur.Phys.J.E*, 4:103, 2001.
35. R.R. Netz and R. Lipowsky. *Phys. Rev. Lett.*, 71:3596–3599, 1993.
36. L. Gao and L. Golubović. *Phys. Rev. E*, 67:021708, 2003.
37. S. K. Sinha, E. B. Sirota, S. Garoff, and H. B. Stanley. *Phys. Rev. B*, 38:2297–2312, 1988.
38. S. K. Sinha. *J. Phys. (France) III*, 4:1543–1557, 1994.